AXISYMMETRIC ELASTIC PROPERTIES OF A SPHERICAL SHELL

PMM Vol. 33, №2, 1969, pp. 280-286
V.I. FEODOS'EV
(Moscow)
(Received July 2, 1968)

The axisymmetrical equilibrium forms of a spherical shell under the action of a uniformly distributed pressure are studied. The deformation is supposed small, but no limitations are imposed on the magnitude of the displacements. The assumptions are exactly those taken in studying flexible rods; this provides the possibility of using terminological analogies.

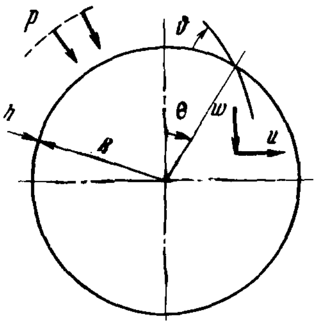

Fig. 1

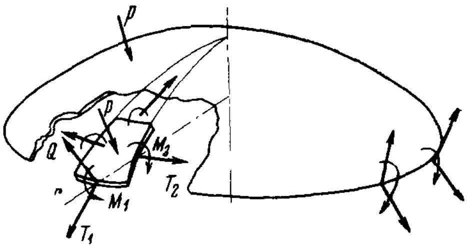

Fig. 2

1. For independent variable we take the angle θ referred to the undeformed surface. We denote by ϑ a positive variation in this angle. We further introduce dimensionless displacements u and w, relative to the shell's radius R (Fig. 1).

From geometrical considerations it follows that:

$$u' = (1+\varepsilon_1)\cos(\theta+\vartheta) - \cos\theta \qquad \left((\;.\;.\;.\;)' = \frac{d(\;.\;.\;.\;)}{d\theta}\right) \tag{1.1}$$
$$w' = (1+\varepsilon_1)\sin(\theta+\vartheta) - \sin\theta$$

$$\varepsilon_2 = \frac{u}{\sin\theta} \tag{1.2}$$

Here ε_1 and ε_2 are strains in the mean surface. At a distance z from the mean surface

$$\varepsilon_{1z} = \varepsilon_1 + \frac{z}{R} R\varkappa_1, \qquad \varepsilon_{2z} = \varepsilon_2 + \frac{z}{R} R\varkappa_2 \tag{1.3}$$

Here

$$R\varkappa_1 = \vartheta' - \varepsilon_1, \qquad R\varkappa_2 = \frac{\sin(\theta+\vartheta)}{\sin\theta} - 1 - \varepsilon_2 \tag{1.4}$$

In accordance with Hooke's law,

$$T_1 = \varepsilon_1 + \mu\varepsilon_2, \qquad M_1 = R\varkappa_1 + \mu R\varkappa_2$$
$$T_2 = \varepsilon_2 + \mu\varepsilon_1, \qquad M_2 = R\varkappa_2 + \mu R\varkappa_1 \tag{1.5}$$

Here T_1, T_2, M_1, M_2 are dimensionless forces and moments

$$T_{1,2} = T_{1,2}^* \frac{1-\mu^2}{Eh}, \qquad M_{1,2} = M_{1,2}^* \frac{12R(1-\mu^2)}{Eh^3}$$

The transverse force Q^* and pressure p reduce to the dimensionless forms

$$Q = Q^* \frac{1-\mu^2}{Eh}, \qquad p_0 = p\frac{R(1-\mu^2)}{2Eh} \tag{1.6}$$

We formulate the three equilibrium equations, neglecting elongations in the mean surface; the first is for the segment of the cap (Fig. 2)

$$T_1 \sin(\theta+\vartheta) - Q\cos(\theta+\vartheta) = -p_0 \sin\theta \tag{1.7}$$

the two others are for an element of this cap (Fig. 2)

$$\alpha^{-1} Q \sin\theta = (M_1 \sin\theta)' - M_2 \cos(\theta + \vartheta) \tag{1.8}$$

$$X' = 2p_0 \sin\theta \sin(\theta + \vartheta) + T_2 \tag{1.9}$$

Here

$$\alpha = h^2 / 12R^2 \tag{1.10}$$

$$X = [T_1 \cos(\theta + \vartheta) + Q \sin(\theta + \vartheta)] \sin\theta \tag{1.11}$$

Equation (1.9) results from equating to zero the sum of all projections of forces onto the r-axis (Fig. 2), perpendicular to the axis of symmetry.

We group the equations obtained into a system suitable for numerical integration

$$u' = (1 + \varepsilon_1)\cos(\theta + \vartheta) - \cos\theta, \qquad \vartheta' = R\varkappa_1 - \varepsilon_1 \qquad X' = 2p_0 \sin\theta\cos(\theta + \vartheta) + T_2,$$

$$(M_1 \sin\theta)' = \alpha^{-1} Q \sin\theta + M_2 \cos(\theta + \vartheta) \qquad w' = (1 + \varepsilon_1)\sin(\theta + \vartheta) - \sin\theta \tag{1.12}$$

The right sides may be computed at each step from Eqs. (1.1)–(1.4), (1.7) and (1.11). The independent variable θ varies from zero to π. At the ends of the interval (at the poles of the spheres) the functions ϑ and u should vanish.

The last of Eqs. (1.12) is integrated independently of the preceding four, and the function w is determined with accuracy up to an arbitrary constant. The following procedure was used to integrate the system (1.11).

2. The system (1.12) has two particular solutions: the first corresponding to a momentless (membrane) state $\vartheta = 0, \quad X = -p_0 \sin\theta\cos\theta, \quad u = -\dfrac{p_0}{1+\mu}\sin\theta, \quad M_1 = p_0$

and the second corresponding to a sphere "turned inside out"

$$\vartheta = -2\theta, \quad X = p_0 \sin\theta\cos\theta, \quad u = \frac{p_0}{1+\mu}\sin\theta, \quad M_1 = -2(1+\mu) - p_0$$

We consider equilibrium forms for which at particular portions of the sphere a linearization of the equations near the first or the second of these particular solutions is admissible. On these portions a numerical integration method may be used.

The remaining interval, if it does not turn out to be too large, may be covered by the method of initial parameters.

We are not able to include all possible equilibrium forms by this procedure; to properly position the sequence of portions spoken of, it is necessary to have some general idea of the shape desired.

We shall effect a linearization near the first particular solution. We set

$$\vartheta = \Delta\vartheta, \qquad X = -p_0 \sin\theta\cos\theta + \Delta X$$

$$u = -\frac{p_0}{1+\mu}\sin\theta + \Delta u, \qquad M_1 = p_0 + \Delta M_1 \tag{2.1}$$

After linearizing all equations we obtain a single fourth order equation for $\Delta\vartheta$

$$\begin{gathered}\Delta\vartheta^{(\mathrm{IV})} + \Delta\vartheta''' \, 2\operatorname{ctg}\theta + \Delta\vartheta'' \left(\frac{p_0}{\alpha} - \frac{2 + \cos^2\theta}{\sin^2\theta}\right) + \\ + \Delta\vartheta' \left[\frac{\cos\theta}{\sin^3\theta}(3 + 2\sin^2\theta) + \frac{p_0}{\alpha}(\operatorname{ctg}\theta - \sin 2\theta)\right] + \\ + \Delta\vartheta \left\{\frac{1-\mu^2}{\alpha} - \frac{3}{\sin^4\theta} - \frac{p_0}{\alpha}[\operatorname{ctg}^2\theta + 2(3+\mu)\cos^2\theta - 1 - 2\mu]\right\} = 0\end{gathered} \tag{2.2}$$

and also

$$\Delta X \alpha^{-1} = \Delta\vartheta'' + \Delta\vartheta' \operatorname{ctg}\theta - \Delta\vartheta(\operatorname{ctg}^2\theta + \mu - p_0/\alpha) \tag{2.3}$$

Here, besides the terms neglected because of the linearization, terms in these last equations of order α are neglected, in comparison with those of order unity.

Near the second particular solution we obtain analogously

$$\vartheta = -2\theta + \Delta\vartheta, \qquad X = p_0 \sin\theta\cos\theta + \Delta X$$

$$u = \frac{p_0}{1+\mu}\sin\theta + \Delta u, \qquad M_1 = -2(1+\mu) - p_0 + \Delta M_1 \tag{2.4}$$

$$\Delta\vartheta^{(IV)} + \Delta\vartheta''' \, 2\mathrm{ctg}\,\theta + \Delta\vartheta''\left(2 + 2\mu - \frac{2+\cos^2\theta}{\sin^2\theta} - \frac{p_0}{\alpha}\right) +$$

$$+ \Delta\vartheta'\left[3\frac{\cos\theta}{\sin^3\theta} + 2(2+\mu)\,\mathrm{ctg}\,\theta + \frac{p_0}{\alpha}(\sin 2\theta - \mathrm{ctg}\,\theta)\right] + \tag{2.5}$$

$$+ \Delta\vartheta\left\{\frac{1-\mu^2}{\alpha} - \frac{3}{\sin^4\theta} - 2(1+\mu)\,\mathrm{ctg}^2\theta + \right.$$

$$\left. + \frac{p_0}{\alpha}\left[\mathrm{ctg}^2\theta - 1 - 2\mu + 2(3+\mu)\cos^2\theta\right]\right\} = 0$$

$$-\Delta X\alpha^{-1} = \Delta\vartheta'' + \Delta\vartheta'\,\mathrm{ctg}\,\theta - \Delta\vartheta\,(\mathrm{ctg}^2\theta - 2 - \mu + p_0/\alpha) \tag{2.6}$$

3. We envisage some typical equilibrium form, such as shown in Fig. 3.

In the interval $(0, \theta_I)$ Eqs. (2.4)–(2.6) are applicable, whereas Eqs. (2.1)–(2.3) apply in the interval (θ_{II}, π). The portion from $\theta = \theta_I$ to $\theta = \theta_{II}$ will be covered by the method of initial parameters.

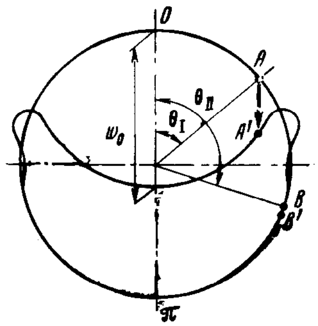

Fig. 3

The size of the intervals changes, depending on the loading parameter p_0. In particualar θ_I may turn out to be zero, or $\theta_{II} = \pi$. Then instead of three portions we have only two; it is important that the interval (θ_I, θ_{II}) not be too large.

Equation (2.5) is integrated under the following boundary conditions: $\Delta\vartheta = 0$, $\Delta X = 0$ for $\theta = 0$;

$$\Delta\vartheta = \Delta\vartheta_I, \ \Delta\vartheta' = \Delta\vartheta_I' \ \text{for} \ \theta = \theta_I$$

where $\Delta\vartheta_I$ and $\Delta\vartheta_I'$ are certain parameters subject to later specification.

As a result of the numerical procedure on the right end of the segment we find the values of the second and third derivatives of the function $\Delta\vartheta$. They depend on $\Delta\vartheta_I$ and $\Delta\vartheta_I'$ linearly. Therefore

$$\Delta\vartheta_I'' = K_1\Delta\vartheta_I + K_2\Delta\vartheta_I', \qquad \Delta\vartheta_I''' = K_3\Delta\vartheta_I + K_4\Delta\vartheta_I' \tag{3.1}$$

where K_i are influence coefficients. They are easily determined after twice solving Eq. (2.5). First we set $\Delta\vartheta_I = 1$ and $\Delta\vartheta_I' = 0$; so that $\Delta\vartheta_I'' = K_1$ and $\Delta\vartheta_I''' = K_3$. In the second integration $\Delta\vartheta_I = 0$ and $\Delta\vartheta_I' = 1$; then $\Delta\vartheta_I'' = K_2$ and $\Delta\vartheta_I''' = K_4$.

For the interval (θ_{II}, π), Eq. (2.2) is used.

For $\theta = \pi$ the function $\Delta\vartheta = 0$ and $\Delta X = 0$. For $\theta = \theta_{II}$ we have, analogously to the first portion,

$$\Delta\vartheta_{II}'' = K_5\Delta\vartheta_{II} + K_6\Delta\vartheta_{II}, \qquad \Delta\vartheta_{II}''' = K_7\Delta\vartheta_{II} + K_8\Delta\vartheta_{II} \tag{3.2}$$

The influence coefficients are determined in the same manner.

We may now pass to integrating (1.12) on the portion (θ_I, θ_{II}). For this we give the values of $\Delta\vartheta_I$ and $\Delta\vartheta_I'$ and from (3.1) determine $\Delta\vartheta_I$ and $\Delta\vartheta_I$. Then with the aid of expressions (1.1)–(1.11) one calculates the values of the functions u, ϑ, X and $M_1 \sin\theta$ at $\theta = \theta_I$. These data are used in a standard Runge-Kutta integration procedure. The integration is carried out up to $\theta = \theta_{II}$ and at the end of the interval we obtain the values of ϑ_k, ϑ_k', X_k and X_k' which are needed for patching with the third part.

At $\theta = \theta_{II}$ we have

$$\vartheta_k = \Delta\vartheta_{II}, \quad X_k = -p_0 \sin\theta_{II}\cos\theta_{II} + \Delta X_{II}$$
$$\vartheta_k' = \Delta\vartheta'_{II}, \quad X_k' = -p_0 \cos 2\theta_{II} + \Delta X'_{II}$$

These conditions guarantee the continuity of all functions at the points where the regions are patched together.

Using Expressions (2.3) and (3.2) and relpacing $\Delta\vartheta'_{II}$ and $\Delta\vartheta_{II}$ by ϑ_k and ϑ'_k, we arrive at two equations

$$X_k + p_0 \sin\theta_{II}\cos\theta_{II} - a\vartheta_k - b\vartheta_k' = 0$$
$$X_k' + p_0 \cos 2\theta_{II} - c\vartheta_k - d\vartheta_k' = 0 \tag{3.3}$$

where

$$a = \alpha\left(K_5 - \operatorname{ctg}^2\theta_{II} + \frac{p_0}{\alpha} - \mu\right), \quad c = \alpha\left(K_7 + K_5 \operatorname{ctg}\theta_{II} + 2\frac{\cos\theta_{II}}{\sin^3\theta_{II}}\right) \tag{3.4}$$
$$b = \alpha\,(K_6 + \operatorname{ctg}\theta_{II}), \qquad d = \alpha\left(K_8 + K_6 \operatorname{ctg}\theta_{II} - \frac{1+\cos^2\theta_{II}}{\sin^2\theta_{II}} + \frac{p_0}{\alpha} - \mu\right)$$

These quantities are calculated by means of the influence coefficients found earlier.

The problem now consists in the choice of initial parameters $\Delta\vartheta_I$ and $\Delta\vartheta_I'$, for which Eqs. (3.3) will be satisfied. This is accomplished in the usual manner, involving linear interpolation with two parameters.

After the quantities $\Delta\vartheta_I$ and $\Delta\vartheta_I'$ are found, a smoothing on two portions is carried out, followed by a final Runge-Kutta integration. As a result we obtain a table of values of ϑ in the interval $(0, \pi)$, and hence the functions u and w, by which the shape of the meridian arcs may be constructed.

4. A few words on the parameters in the numerical realization of the described algorithm.

The interval of integration $(0, \pi)$ was divided into 255 pieces. Thus the functional values at 256 points were considered. The increment size $\pi/255$ was kept fixed in all three portions.

A central finite difference scheme was used and two extra points were introduced at each end of the intervals of numerical integration.

The positions of the boundaries, θ_I and θ_{II}, were chosen by the computer according to the condition $|\Delta\vartheta| < 0{,}06$.

In regions with small angle θ (in the shallow parts of the sphere) the admissibility of linearization is determined not only by the magnitude of the rotation angle $\Delta\vartheta$, but also by the magnitude of the angle θ; hence for the regions adjacent to the poles one imposes an additional condition

$$\frac{|\Delta\vartheta|}{2\theta} < 0.06, \qquad \frac{|\Delta\vartheta|}{2(\pi-\theta)} < 0.06$$

As for the choice of initial parameters $\Delta\vartheta_I$ and $\Delta\vartheta_I'$, the necessary accuracy was considered attained, if in two successive linear interpolations, the changes in $\Delta\vartheta_I$ and $\Delta\vartheta_I'$ in absolute value were simultaneously less than 0.0001.

After this, by way of various tests, the solution was found for a certain initial value of p_0, and the computer carried out a search for new $\Delta\vartheta_I$ and $\Delta\vartheta_I'$ admitting variable values of $p_0 + \Delta p_0$ and for fixed θ_I and θ_{II}. Then these latter were determined in accordance with the condition indicated, and the solution again constructed. The quantity Δp_0 was adjusted by hand depending on the circumstances, since it was very difficult to specify beforehand the principles in the choice of the increments Δp_0.

If the domain of the desired parameters $\Delta\vartheta_I$ and $\Delta\vartheta_I'$ is known sufficiently accurately, then the computer time involved in determining the equilibrium form will be very moderate. But in a transition through the extremal points p_0^{max} or p_0^{min} the computer naturally lost the basic values of the parameters and required a fairly long time to set up the computation process anew. This was done with the aid of auxiliary programs.

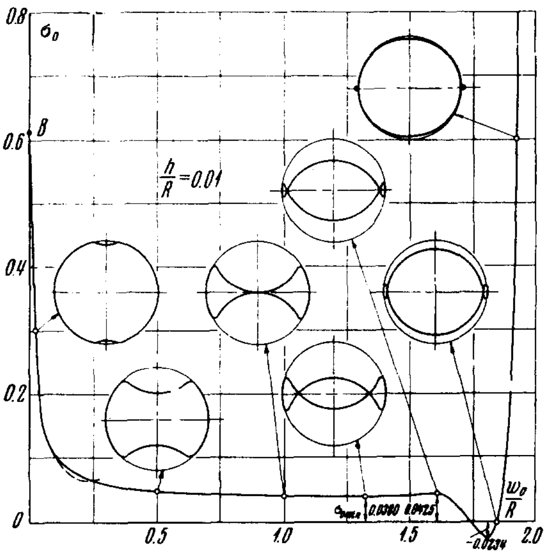

Fig. 4

5. First were considered equilibrium forms symmetric with respect to the equatorial plane. It was supposed that two depressions formed simultaneously at opposite poles of the sphere, and then moved toward each other. The computations were taken only for one of the hemispheres. For $\theta = {}^1/_2\pi$, $X = 0$ and $\vartheta = 0$.

The results of the computation are given in Fig. 4. The abscissa measures the dimensionless displacement of the pole w_0 / R, relative to the equatorial plane; and the ordinate is the loading parameter

$$\sigma_0 = \frac{p}{E}\frac{R^2}{2h^2}$$

The left part of the "load-displacement" diagram is a straight line passing through the origin. The deformation in this region is conditioned only by the contraction of the shell as a whole, and the displacement is very small. Within the accuracy limits of the diagram, this straight line lies on the ordinate axis.

The graph indicates the bifurcation point B. From it the curve sharply drops down and σ_0 has two minima at

$w_0 / R = 1.32 \qquad (\sigma_0 = 0.0380)$
$w_0 / R = 1.80 \qquad (\sigma_0 = -0.0234)$

and a maximum at

$w_0 / R = 1.61 \qquad (\sigma_0 = 0.0425)$

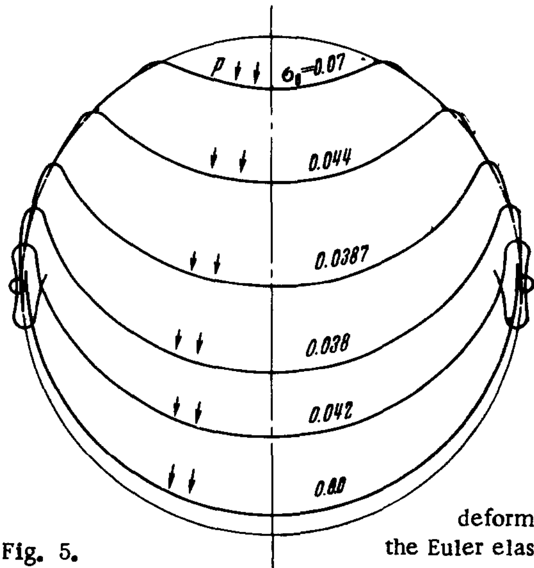

Fig. 5.

The shapes of the meridian arcs on the deformed shell are also shown in Fig. 4. As in the Euler elastic properties, no limitations are imposed as regards self-intersections of the surface. Fig. 5 shows the equilibrium shapes in a coarser scale. All calculations were carried out with $h/R=0.01$.

Equilibrium forms asymmetrical with respect to the equatorial plane were also considered; they were obtained by integrating the equations throughout the interval $(0, \pi)$. The load-displacement diagram is shown in Fig. 6. Here the quantity w_0/R represents the mutual displacement of the poles. The loading has one minimum at $w_0/R = 1.3$ ($\sigma_0 = 0.0381$).

The construction of the right part of the diagram for $w_0 / R > 3$ encountered great difficulty. The zone θ_{II}, π (Fig. 3) is rapidly reduced, and the nonlinearizable portion

(θ_I, θ_{II}) (Fig. 3) increases to such an extent that the method of initial parameters is inapplicable.

The equilibrium forms of the shell for various values of σ_0 are shown in Fig. 7. The lower pole of the sphere is taken as fixed.

Comparing the diagrams shown in Figs. 4 and 6, it is seen that for $w_0 / R < 1$ they coincide; the deformations of the upper and lower hemispheres practically do not influence one another.

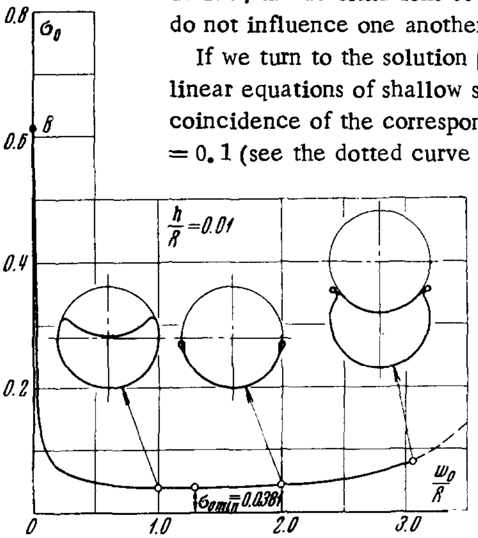

Fig. 6

If we turn to the solution [1] obtained earlier on the basis of the nonlinear equations of shallow shell theory, then we discover there also a coincidence of the corresponding curves, but only up to the value $w_0 / R = 0.1$ (see the dotted curve in Fig. 4). The value $\sigma_0^{min} = 0.06$ found earlier does not agree with the new value $\sigma_0^{min} = 0.038$. This is a natural consequence of the error contained in the shallow shell equations.

It is interesting to consider the results of the numerical solution near the point of bifurcation.

Fig. 8 shows, in a different scale, the left potion of the diagram $\sigma_0 = f(w_0 / R)$ (Figs. 4 and 6).

The line passing through the origin characterizes the displacement of the shell due to uniform compression. The curve dropping down from the point of bifurcation B corresponds to bent equilibrium shapes.

Since the indentation near the pole was small, the interval of integration was divided into two rather than three zones. On the part from $\theta = 0$ to $\theta = 0.5$ the nonlinear equations (1.12) were integrated by the Runge-Kutta method, and from $\theta = 0.5$ to $\theta = \pi$ the linearized equations (2.2) and (2.3) were solved by the method used before on the third portion. As is clear from Fig. 8, the curve and the straight line intersect at B at a certain angle. The line on the left reveals no new equilibrium forms.

In connection with this a very interesting question arises. Near the bifurcation point, how are the linear and nonlinear solutions to be joined, and how valid is linearization of the equations near the pole?

On the one hand, there is an analytic solution of the problem in the linear framework, which for a spherical shell yields a loss of stability with resulting configuration in the form of a Legendre function $w / R = CP_n(\theta)$ (with $h / R = 0.01$ $n = 18$). The indeterminate multiplier C may be either positive or negative.

On the other hand, the numerical solution of the nonlinear equations near the bifurcation point gives only a positive value for the deflections (into the sphere).

The answer to the question posed may apparently be given only on the basis of an analytical investigation of the equation with small nonlinearity. A numerical solution here may not be effected. As an approximation, it looses accuracy at the bifurcation point since the scale of the function w / R becomes vanishingly small; in fact the critical load itself may not be determined sufficiently accurately because of the very sharp angle between the straight line and the curve. Thus with the numerical procedure used, there appears already at $\sigma_0 = 0.62$ a small ($w_0 / R = 0.000353$) but decisive expression for the bent equilibrium shape, near to the Legendre function P_{18} (θ). For $\sigma_0 \geqslant 0.63$ the computer consistently yielded, with accuracy of 0.07%, a displacement w_0 / R corresonding to uniform compression of the sphere.

Thus, in distinction to the known linear solution, which gives a critical value of $\sigma_0 = 0.605$, here we obtain a value of σ_0 lying in the interval (0.62, 0.63). Such a discrepancy is not significant. It easily may be dis-

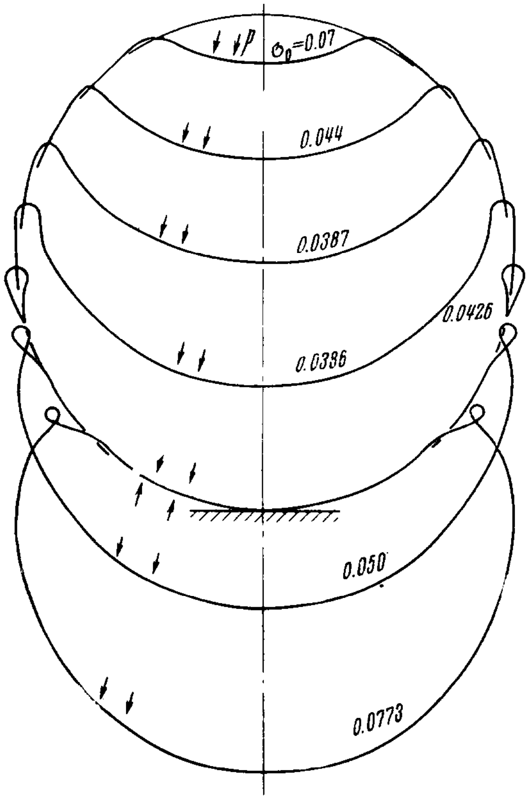

Fig. 7

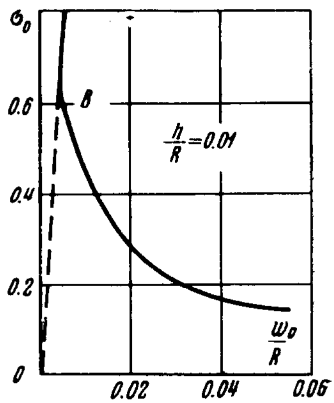

Fig. 8

missed on account of the normally admissible differences in the description of the original equations of stability, and on account of the obvious difficulties in the approach to the bifurcation point. In any case this question needs deeper study.

The results obtained in this paper do not exhaust the possible equilibrium forms for a spherical shell. The number of such forms is apparently very large, and there arises a natural fear that upon deeper analysis of the exotic aspects of the nonuniqueness questions arising from the nonlinear problem, the number will grow into a cursed manifold.

In conclusion the author feels obliged to express deep thanks to the personnel of the computing center for their tolerant attitude toward the restive author. Particular help was shown by Z. A. Kudlai and M. I. Neretin, whose services guaranteed uninterrupted functioning of the computers.

BIBLIOGRAPHY

1. Gabril'iants, A. G. and Feodos'ev, V. I., Axially-symmetric forms of equilibrium of an elastic spherical shell under uniformly disturbed pressure. PMM Vol. 25, №6, 1961.

Translated by P. F.